JPn Neuroscience
The Journal of Physiology

K_{ATP} channels in the nodose ganglia mediate the orexigenic actions of ghrelin

Gintautas Grabauskas, Xiaoyin Wu, Yuanxu Lu, Andrea Heldsinger, Il Song, Shi-Yi Zhou and Chung Owyang

Division of Gastroenterology, Department of Internal Medicine, University of Michigan Health System, Ann Arbor, MI, USA

Key points

- Ghrelin, a hunger signalling peptide derived from the peripheral tissues, overcomes the satiety signals evoked by anorexigenic molecules, such as cholecystokinin (CCK) and leptin, to stimulate feeding.
- Using *in vivo* and *in vitro* electrophysiological techniques, we show that ghrelin hyperpolarizes neurons and inhibits currents evoked by leptin and CCK-8.
- Administering a K_{ATP} channel antagonist or silencing Kir6.2, a major subunit of the K_{ATP} channel, abolished ghrelin inhibition.
- The inhibitory actions of ghrelin were also abolished by treating the vagal ganglia neurons with pertussis toxin, as well as phosphatidylinositol 3-kinase (PI3K) or extracellular signal-regulated kinase 1 and 2 (Erk1/2) small interfering RNA.
- Feeding experiments showed that silencing Kir6.2 in the vagal ganglia abolished the orexigenic actions of ghrelin.
- These data indicate that ghrelin modulates vagal ganglia neuron excitability by activating K_{ATP} conductance via the growth hormone secretagogue receptor subtype 1a–$G_{\alpha i}$–PI3K–Erk1/2–K_{ATP} pathway.
- This provides a mechanism to explain the actions of ghrelin with respect to overcoming anorexigenic signals that act via the vagal afferent pathways.

Abstract Ghrelin is the only known hunger signal derived from the peripheral tissues. Ghrelin overcomes the satiety signals evoked by anorexigenic molecules, such as cholecystokinin (CCK) and leptin, to stimulate feeding. The mechanisms by which ghrelin reduces the sensory signals evoked by anorexigenic hormones, which act via the vagus nerve to stimulate feeding, are unknown. Patch clamp recordings of isolated rat vagal neurons show that ghrelin hyperpolarizes neurons by activating K^+ conductance. Administering a K_{ATP} channel antagonist or silencing Kir6.2, a major subunit of the K_{ATP} channel, abolished ghrelin inhibition *in vitro* and *in vivo*. Patch clamp studies show that ghrelin inhibits currents evoked by leptin and CCK-8, which operate through independent ionic channels. The inhibitory actions of ghrelin were abolished by treating the vagal ganglia neurons with pertussis toxin, as well as phosphatidylinositol 3-kinase (PI3K) or extracellular signal-regulated kinase 1 and 2 (Erk1/2) small interfering RNA. *In vivo* gene silencing of PI3K and Erk1/2 in the nodose ganglia prevented ghrelin inhibition of leptin- or CCK-8-evoked vagal firing. Feeding experiments showed that silencing Kir6.2 in the vagal ganglia abolished the orexigenic actions of ghrelin. These data indicate that ghrelin modulates vagal ganglia neuron excitability by activating K_{ATP} conductance via the growth hormone secretagogue receptor subtype 1a–$G_{\alpha i}$–PI3K–Erk1/2–K_{ATP} pathway. The resulting hyperpolarization renders the neurons less responsive to signals evoked by anorexigenic hormones. This provides a mechanism to explain the actions of ghrelin with respect to overcoming anorexigenic signals that act via the vagal afferent pathways.

DOI: 10.1113/JP270788

(Resubmitted 22 April 2015; accepted after revision 26 June 2015; first published online 15 July 2015)
Corresponding author C. Owyang: 3912 Taubman Center, SPC 5362, 1500 East Medical Center Drive, University of Michigan Health System, Ann Arbor, MI 48109, USA. Email: cowyang@med.umich.edu

Abbreviations CCK, cholecystokinin; DMEM, Dulbecco's modified Eagle medium; EGFP, enhanced green fluorescent protein; Erk1/2, extracellular signal-regulated kinase 1 and 2; Cy3, cyanine 3; FBS, fetal bovine serum; GSH-R1a, growth hormone secretagogue receptor subtype 1a; MAPK, mitogen-activated protein kinase; PI3K, phosphatidylinositol 3-kinase; PKA, protein kinase A; PKC, protein kinase C; PLC, phospholipase C; PTx, pertussis toxin; siRNA, small interfering RNA; SOCS3, suppressor of cytokine signalling 3.

Introduction

Ghrelin, which is released from gastric X/A-like (P/D1 in humans) endocrine cells in response to fasting, is important in the regulation of feeding behaviour (Kojima *et al.* 1999; Gnanapavan *et al.* 2002). Ghrelin is the only known hunger-generated signal derived from the peripheral tissues. Peripheral administration of ghrelin in animals stimulates food intake and increases acid and protein secretion. It also increases gastric motility but inhibits lipid metabolism (Tschöp *et al.* 2002; Nakazato *et al.* 2001; Li *et al.* 2006; Tack *et al.* 2006; Kobashi *et al.* 2009).

Ghrelin signalling involves activation of the growth hormone secretagogue receptor subtype 1A (GHS-R1a) (Kojima *et al.* 1999), whose mRNA is expressed in the neuron bodies of the vagal sensory ganglia (Sakata *et al.* 2003). Kentish *et al.* (2011) traced vagal afferents anterogradely to their terminals in the gastric mucosa, and showed them to be in close apposition to ghrelin-containing cells, suggesting that ghrelin signals from the stomach are transmitted to the brain via the vagus nerve (Date *et al.* 2002). Moreover, peripherally administered ghrelin diminishes vagal afferent activity, whereas vagotomy or perivagal capsaicin abolishes facilitation of feeding in both rodents and humans (Date *et al.* 2002; 2005; le Roux *et al.* 2005). However, other studies have shown that ghrelin acts in preautonomic hypothalamus as well as in vagal brainstem nuclei to modulate pancreatic secretion, gastric motility and feeding (Dickson & Luckman, 1997; Li *et al.* 2006; Cui *et al.* 2011; Swartz *et al.* 2014). These discrepancies may be a result of differences in animal species and/or experimental conditions. It is also conceivable that these different sites may mediate the different actions of ghrelin. It has been suggested that ghrelin acts via vagal afferent pathways to modulate satiety, whereas the hypothalamic receptors of ghrelin probably regulate long-term feeding behaviour and energy metabolism (Schwarz *et al.* 1996).

Similar to the studies reported by Nakazato *et al.* (2001), our preliminary studies demonstrate that ghrelin mainly acts via vagal afferent pathways to modulate satiety. Cholecystokinin (CCK) (Smith *et al.* 1985) and leptin (Barrachina *et al.* 1997) are also known to act via vagal sensory pathways to regulate feeding. Ghrelin is reported to reduce the satiety signal evoked by anorexigenic molecules, such as leptin (Nakazato *et al.* 2001; Noqueiras *et al.* 2004) and CCK (DeLartigue *et al.* 2012), which act on the nodose ganglia to modulate feeding.

The mechanisms by which ghrelin exerts its inhibitory effects on leptin and CCK are unknown. Because leptin and CCK act via diverse signal transduction pathways (Heldsinger *et al.* 2011) to activate nodose ganglia firing, it is improbable that ghrelin acts by interrupting these diverse signalling cascades. We propose that ghrelin activates an intracellular transduction pathway altering the electrophysiological properties of the nodose ganglia, rendering it less responsive to anorexigenic peptide stimulation.

K_{ATP} channels couple metabolism to electrical activities (Proks & Ashcroft, 2009). An increased blood glucose level leads to channel closure, membrane depolarization and enhanced electrical activity (Grabauskas *et al.* 2010; 2013). Conversely, a decreased glucose concentration opens K_{ATP} channels and reduces neuronal firing (Levin, 2001; Browning, 2013). It is conceivable that ghrelin regulates nodose ganglia responsiveness to anorexigenic signals through the opening of K_{ATP} channels in the nodose ganglia.

In the present study, we define a mechanism used by ghrelin to modulate the excitability of the vagal nodose ganglia, resulting in enhanced feeding. Western blotting, patch clamp electrophysiological studies and gene silencing techniques in cultured rat nodose ganglia neurons, as well as *in vivo* single-cell electrical recordings and feeding studies, show that ghrelin modulates the excitability of vagal nodose ganglia by activating a K_{ATP} conductance via the GSH-R1a–$G_{\alpha i}$–phosphatidylinositol 3-kinase (PI3K)–extracellular signal-regulated kinase 1 and 2 (Erk1/2)–K_{ATP} pathway. This results in increased feeding.

Methods

Ethical approval

All animal procedures were performed in accordance with National Institutes of Health guidelines and with the approval of the University Committee on Use and Care of Animals at the University of Michigan.

Retrograde tracing

Five Sprague–Dawley male rats (200 g; Harlan Laboratories, Indianapolis, IN, USA) were deeply anaesthetized with a mixture of isoflurane in air as described previously (Grabauskas *et al.* 2010). Following laparotomy, crystals of the retrograde tracer 1,1′-dioctadecyl-3,3,3′,3′-tetramethylindocarbocyanine perchlorate (DiI; Life Technologies, Invitrogen, Grand Island, NY, USA) were applied to the duodenum. To confine the dye to the application site, the DiI crystals were embedded in a fast curing epoxy resin that was allowed to harden for approximately 5 min. The surgical area was then washed with warm sterile saline, and the wound was closed with nylon sutures (4-0). Analgesic buprenophrine (0.3 mg kg^{-1}) was administered. Each animal was housed in a separate cage. After surgery, the animals were monitored daily for signs of stress, including adaptation of a crouched posture, changes in appearance of hair and weight loss. Ten to 15 days after the recovery period, the animals were humanely killed by CO_2 asphyxiation and the nodose ganglia were dissected. In a separate study, we labelled neurons with fibres projecting deep into the lung to compare duodenal and pulmonary innervating neurons. Five Sprague–Dawley male rats (200 g; Harlan Laboratories) were deeply anaesthetized with a mixture of isofluorane and then given transdermal injections of 5% DiI (10 μl) into the right and left lungs using a 50 μl Hamilton syringe. Postmortem analysis showed diffusion of the dye into the large bronchi and vessels in three of five animals. The animals were humanely killed by CO_2 asphyxiation, 7–14 days postinjection. Retrogradely labelled nodose ganglia neurons were identified using a Ti microscope (Nikon, Tokyo, Japan) equipped with a tetramethylrhodamine epifluorescence filter.

Isolation and culture of vagal sensory neurons

Sprague–Dawley rats (160–240 g; Harlan Laboratories) were killed by CO_2 asphyxiation and the nodose ganglia were dissected and placed in a 35 mm culture dish containing Ca^{2+}- and Mg^{2+}-free Hanks' balanced salt solution with penicillin and streptomycin (Heldsinger *et al.* 2011). Desheathed ganglia were sliced into small fragments and placed in a 1.5 ml centrifuge tube containing digestion buffer (dispase II; Roche Diagnostics, Life Science, Indianapolis, IN, USA) and collagenase IA (Life Technologies, Invitrogen) (1 mg ml^{-1}). After incubation at 37°C for 60 min, cells were dispersed by gentle trituration through Pasteur pipettes and washed in Dulbecco's modified Eagle medium (DMEM; Life Technologies, Invitrogen). The cells were resuspended in L-15 medium (Life Technologies, Invitrogen) containing 10% fetal bovine serum (FBS), plated onto poly-L-lysine-coated (100 μg ml^{-1}) coverslips for 30 min and cultured in DMEM with 10% FBS at 37°C. Neurons were stuck to coverslips and maintained in culture for 16–48 h at 37°C before recording.

Neuron transfection with small interfering RNA (siRNA)

Primary vagal ganglia neuronal cultures were supplemented with (1.5 mg ml^{-1}) of siRNA Kir6.2 (sc-42629), Erk1 (sc-156030), Erk2 (sc-156031), PI3K (si156021) and random siRNA (sc-37007) (Santa Cruz Biotechnology, Dallas, TX, USA) at 37°C (Heldsinger *et al.* 2011). To aid in the identification of transfected neurons, siRNAs were conjugated with cyanine 3 (Cy3) or FITC fluorescent label. Duplex siRNAs were labelled with the method described in the Silencer siRNA labelling kit (Life Technologies, Ambion, Austin, TX, USA). Patch clamp recordings were conducted only on neurons positively identified as containing Cy3 or FITC label. After 3 h, media containing siRNA were aspirated and replaced with DMEM/F-12 media containing 100 mg dl^{-1} glucose and 10% FBS supplemented with gentamycin (100 U ml^{-1}). The neurons were cultured for 72–96 h at 37°C in a 5% CO_2 atmosphere. Whole-cell patch clamp recordings were performed on cultured vagal sensory neurons within 72–96 h after siRNA transfection of enhanced green fluorescent protein (EGFP)-positive neurons.

Whole-cell patch clamp electrophysiology

All measurements were made in a physiological saline solution composed of (in mM): 140 NaCl, 5 KCl, 2 $CaCl_2$, 1 $MgCl_2$, 5 glucose and 10 HEPES; pH adjusted to 7.3 with NaOH (Grabauskas *et al.* 2010). Whole-cell recordings were acquired using borosilicate glass electrodes with resistance between 3 and 6 MΩ (A-M Systems,Sequim, WA, USA) backfilled with a saline solution composed of (in mM): 130 potassium gluconate, 10 HEPES, 10 EGTA, 1.0 $MgCl_2$, 2.5 $CaCl_2$, 1.0 ATP and 0.3 GTP; pH adjusted to 7.3 with KOH. Current and voltage recordings were acquired from discrete isolated vagal sensory neurons using an Axopatch 200B Amplifier (Molecular Devices, Sunnyvale, CA, USA) filtered at 2 kHz using a four-pole low-pass Bessel filter. For data analysis, signals were digitized using an analog-to-digital converter (Axon Digidata 1322B; Molecular Devices), stored and analysed on a personal computer running pCLAMP 9 software (Molecular Devices). The input resistance was calculated by measuring the neuron membrane potential displacement from –60 mV in response to a –10 pA current pulse.

Western blotting

Vagal ganglia neurons were isolated and harvested in accordance with a technique described previously

(Heldsinger *et al.* 2011). Briefly, the neurons were incubated with inhibitors for 30 min before a 10-min stimulation with ghrelin. The reaction was stopped by the addition of 1 ml of chilled PBS buffer. After washing, lysis buffer (30 μl) with protease inhibitor (Roche Diagnostics, Life Science) was added to the culture dish and the cells were incubated for 15 min at 4°C. The lysate was centrifuged at 14,000 *g* for 10 min. Protein samples were then run on 12% Ready Gel Tris-HCl (Bio-Rad Laboratories, Hercules, CA) for 1.5 h at 80 V. Proteins were then transferred to PVDF membranes for 1 h at 80 V. The membranes were blocked with StartingBlock T20 blocking buffer (Life Technologies, Waltham, MA, USA) at room temperature, probed with primary antibodies against Erk1/2 (Cell Signaling Technology, Danvers, MA, USA), phosphorylated-Erk1/2 (Cell Signaling Technology), phospho-PI3K (Cell Signaling Technology) and GAPDH (Santa Cruz Biotechnology) at a dilution of 1:1000 at 4°C overnight, and then washed in Tris-buffered saline for 1 h. The membranes were probed with corresponding horseradish peroxidase-conjugated secondary antibodies at a dilution of 1:2000. The resulting bands were scanned with an Epson Stylus Photo R2400 (Epson Corp., Long Beach, CA, USA) and analysed using ImageJ (NIH, Bethesda, MD, USA).

Peptides and drugs

Ghrelin, leptin and CCK-8 (R&D Systems, Minneapolis, MN, USA) were prepared on the day of the experiment by diluting 50 μl aliquots of 10^{-5} M stock solution. For western blotting, the role of $G_{\alpha i/o}$ G protein-coupled receptors in the signalling process was examined by overnight treatment of neurons with 1 μl ml^{-1} pertussis toxin (PTx), a bacterial toxin that catalyzes G protein heterotrimer interaction with receptors. For electrophysiology studies, PTx was included in the recording electrode internal solution before ghrelin stimulation (Barbier & Cortina 1988; Grabauskas *et al.* 2007). A phospholipase C (PLC) inhibitor U73122 (10 μM) was used to examine the involvement of PLCs (Yule & Williams, 1992). The non-selective protein kinase inhibitor H7 (30 μM; R&D Systems) was used to determine whether protein kinases play a role in mediating the actions of ghrelin (Quick *et al.* 1992). Similarly, SQ 22536, an adenylate cyclase inhibitor (100 μM; R&D Systems) (Heldsinger *et al.* 2014), was used to clarify the role of adenylate cyclase in the mediation of ghrelin signalling. Calphostin C, a protein kinase C (PKC) agonist (1 μM, R&D Systems) (Au *et al.* 2006; Grabauskas *et al.* 2007), was used to determine whether PKC plays a role. Wortmannin (100 nM; R&D Systems) was used to inhibit P13K (Heldsinger *et al.* 2011). All agonists, antagonists and their controls were prepared on the day of the experiment by diluting stock solutions stored at appropriate temperatures. The concentrations of the chemicals used were those shown to be effective in the literature cited.

RT-PCR

RNA was extracted from the vagal ganglia using TRIzol (Life Technologies, Ambion), in accordance with the manufacturer's instructions. Reverse transcription was performed using 5 μg of total RNA. The resultant cDNAs were used for PCR with primer sets targeting Kir6.2 (sense: AGACCACCAGCCCGGAGGGCG, antisense GG GCACTTTAACGGTGTTCCC; GenBank accession number NM_031358), Erk1 (sense: GGCTGCATTCTGGCT GAGATG-3, antisense: CTCCATGTCAAAGGTGAATGG, GenBank accession number NM_053842), Erk2 (sense: TCGTACATCGGAGAAGGCGCC, antisense: TAATTTC TGGAGCTCTGTACC, GeneBank accession number NM_053842), PI3K (sense: ACCTGTTAGGGATTCTA GCCC, antisense: TGTCGTAACTCTGCAGGGTT, GenBank accession number NM_013005) and GAPDH (sense: CACCACCATGGAGAAGGCTGG, antisense: GGGCACTTTAACGGTGTTCCC, GenBank accession number AF_106860). GAPDH served as an internal control. PCR was performed with Taq DNA polymerase (Promega, Madison, WI, USA) through 30 cycles of denaturation (30 s at 94°C), annealing (30 s at 50°C) and extension (30 s at 72°C), followed by final extension (10 min at 72°C). The PCR products were loaded in a 1.2% Tris-borate-EDTA-buffered agarose gel, and the bands were visualized after gel electrophoresis by ethidium bromide staining and UV light illumination. The resulting bands were scanned with an Epson Stylus Photo R2400 (Epson Corp.) and analysed using ImageJ (NIH).

siRNA and *in vivo* electroporation

Kir6.2 (sc-42629), Erk1 (sc-156030), Erk2 (sc-156031), PI3K (si156021) and random siRNA (sc-37007) were purchased from Santa Cruz Biotechnology. The pEGFP-N1 vector (BD 6085-1), which encodes the *Aequorea victoria* GFP, was purchased from BD Biosciences (San Jose, CA, USA). The *in vivo* electroporation was performed as described previously (Saito *et al.* 2006; Zhou *et al.* 2011). Each rat was anaesthetized and placed supine on a custom-made surgical plate. Body temperature was maintained at 37 ± 1°C with a homeothermic blanket system (Harvard Bioscience, Holliston, MA, USA) as described previously (Fan *et al.* 2009). The vagal nodose ganglia were exposed by way of a ventral approach. The incision was made from the midline of the neck. With the use of a surgical operating microscope, the caudal end of the ganglion with the attached vagus nerve was

separated from the adjacent cervical sympathetic trunk and carotid artery. The vagus ganglion was carefully isolated, and the area was moistened with saline. A piece of filter paper soaked with protease (type XIV, 0.3 mg ml^{-1}) was applied to the ganglion for 15 min. A bevelled glass micropipette with tip diameter 35–45 μm (Clunbury Scientific, Bloomfield Hills, MI, USA) was filled with a 2:1 mixture of Kir6.2, PI3K, Erk1 and Erk2 siRNA (10 μM; 14 μl^{-1}) or control siRNA (10 μM; 14 μl^{-1}) with pEGFP-N1 vector (1 $\mu g\ \mu l^{-1}$; 7 μl). The micropipette, connected to a nanopump (PV830 Pnematic PicoPump; World Precision Instruments, Sarasota, FL, USA), was guided by a micromanipulator through a small incision on the surface of the nodose ganglion. siRNAs and pEGFP-N1 vector were then injected into the left and right vagal ganglia (bilateral; 20 nl each). The micropipette was left in the ganglion for 10 min and then slowly withdrawn. A pair of stainless steel electrodes was placed on the ganglion 15 min after the injection. The gap between the electrodes was fixed at 2 mm. Square-wave electric pulses were delivered by an isolated pulse stimulator (Model 2100; A-M Systems). A train of square-wave pulses with pulse duration of 20 ms was delivered at 50 V cm^{-1} at a frequency of 1 Hz, followed by the same stimulation with the opposite polarity. In a separate study, a control group of animals was treated with bilateral electroporation of a mixture of control siRNA (Santa Cruz Biotechnology) and pEGFP-N1. Transfection efficiency was assessed by measuring GFP expression, specific protein immunoreactivity, mRNA expression and protein expression. GFP expression, which is a novel genetic reporter system, was measured using fluorescence microscopy with excitation at 488 nm. Because the specific target siRNA construct was packaged with GFP reporter gene, the distribution of siRNA expression and GFP expression probably overlaps. Research has shown that transfection of siRNA into neurons in the CNS has a maximal effect 3–6 days post-transfection, with silencing lasting up to 2 weeks. Studies were performed 5 days after electroporation. We determined the optimal conditions for electroporation and GFP expression in accordance with the parameters: voltage (1–80 V), duration (5–120 ms), pulse number (1–12 times) and frequency of pulse delivery (0.5–10 Hz). The optimal stimulation paradigm was 50 V cm^{-1} with 10 pulses delivered at 1 Hz (20 ms duration). These parameters were most effective to reduce the targeted gene expression in the vagal sensory ganglia with the least cell damage.

Recording of single-unit vagal sensory neuronal activity

The animals were anaesthetized with a mixture of xylazine and ketamine (13 and 87 mg kg^{-1} body weight, respectively). Our data show that this anaesthesia was associated with significant increase in blood glucose concentration to 220 mg dl^{-1}. To investigate the possible interference of elevated blood glucose on the electrophysiological recording, we performed similar single-unit recordings in rats anaesthetized with phenobarbital, which has no effect on blood glucose ($n = 4$). We showed that the neuronal responses to CCK-8 and leptin stimulation remained the same as those observed in rats anaesthetized with xylazine and ketamine. Recording of single-unit vagal sensory activity was performed as described previously by Li *et al.* (1999). Supplemental doses of the anaesthetic agents were administered as needed to maintain a deep level of anaesthesia and muscle relaxation. The animals were ventilated with a respirator, and a tracheal tube permitted artificial ventilation with room air (75–85 strokes min^{-1}; tidal volume 3.5–4.0 cm^3). Rats were placed in a small animal stereotaxic frame (David Kopf Instruments, Tujunga, CA, USA). Body temperature was maintained with a special heating pad. The right vagal sensory ganglion was exposed by a short dorsal approach. The bevelled glass micropipette filled with 1.0 M KCl and neurobiotin tracer (0.2%; Vector Laboratories, Burlingame, CA, USA) was lowered into the nodose ganglion. A reference electrode was placed on a skin incision near the recording electrode. Neuronal discharges recorded were amplified by a high-input impedance preamplifier (A-M Systems), monitored with an oscilloscope and audio monitor and displayed, and then stored on a computer using Axon tape software (Molecular Devices).

Juxtacellular labelling and histological identification of recorded neurons

On completion of the single-unit recording experiment, recorded neurons were labelled by injecting neurobiotin using the technique of juxtacellular iontophoresis (Gao *et al.* 2006). Continuous electrophysiological control ensured the viability of the neurons. The electrode was positioned as close to the recorded neuron as possible. Using the bridge circuit of the recording amplifier, the marker was applied in pulses (250 ms on and 250 ms off). The intensity of the DC current was gradually increased from 2 to 8 nA.

Immunocytochemistry

Immunocytochemistry studies to localize the inwardly rectifying Kir6.2 (Santa Cruz Biotechnology), Erk1/2 (Cell Signaling Technology) and GSH-R1a (Santa Cruz Biotechnology) were performed on vagal sensory neurons as described previously (Helsinger *et al.* 2012). Following anaesthesia with urethane, a transcardial perfusion was

performed with ice-cold heparinized PBS and subsequently with fixative containing 4% paraformaldehyde, 0.2% picric acid and 0.35% glutaraldehyde in phosphate buffer (0.1 mol l^{-1}, pH 7.4). The left and right vagal sensory ganglia were removed and placed in the same fixative for 2 h at room temperature and then in 25% sucrose in PBS (0.1 mol l^{-1}) overnight at 4°C. The ganglia were cut into 5 μM longitudinal sections using a precision cryostat (Leica Microsystems, Wetzlar, Germany). The sections were collected in serially ordered sets, thaw-mounted on gelatin-chromium coated slides and stored at −70°C. For permeabilization and background reduction, sections of the vagal ganglia were incubated in 5% normal donkey serum in PBS for 1 h at room temperature. Staining was performed using the primary antibodies against Kir6.2, Erk1/2 and GSH-R1a (all at a dilution of 1:200). The primary antibodies were diluted in PBS containing 2% normal donkey serum, 0.3% Triton X-100 and 0.1% sodium azide. Tissues were incubated overnight at room temperature, washed in PBS and then exposed for 1 h to species-specific Alexa Fluor 488- (Life Technologies, Molecular Probes) and Cy3-conjugated secondary antibodies (Jackson ImmunoResearch Laboratories, West Grove, PA, USA) and AMCA streptavidin (Vector Laboratories) diluted in PBS containing 0.3% Triton X-100 (dilution 1:200). The sections were coverslipped and sealed. The specificity of antibodies was demonstrated by excluding the primary antibodies or secondary antibodies during the staining procedure, which resulted in complete abolition of staining of the vagal ganglia. All preparations were examined with a BX51 epifluorescence microscope (Olympus, Tokyo, Japan) equipped with a digital camera. The images were analysed by using filter combinations that enabled separate visualization of multiple fluorophores. Images were stored and analysed with Image-Pro Plus software (Media Cybernetics, Rockville, MD, USA) or Photoshop CS2 (Adobe Systems, San Jose, CA, USA). The digital images taken by the confocal microscope were analysed with LSM Image Browser (Carl Zeiss, Oberkochen, Germany) and Photoshop CS2 (Adobe Systems).

Food intake studies and effects of electroporation with Kir6.2 siRNA

Before starting the food intake studies, the rats were randomly divided into two groups of five rats each and the right and left nodose ganglion were electroporated with random siRNA (sc-37007) or Kir6.2 siRNA (sc-42629; Santa Cruz Biotechnology). Feeding studies were initiated 5 days after electroporation. The rats were starved overnight (12 h) with free access to water. On the day of the experiment, the control rats were given a saline injection and the study rats were given an injection of ghrelin (25 μg kg^{-1} I.P.). The feeding study was initiated at 09.00 h. The rats were given weighed food and their cumulative food intake was recorded at 1 h intervals over 3 h, as described by Schwartz *et al.* (1996).

Statistical analysis

All data are expressed as the mean ± SEM. $P < 0.05$ was considered statistically significant (two-way anova or Fisher's exact test). All statistical analyses were performed using InStat (GraphPad Software, San Diego, CA, USA).

Results

Ghrelin inhibits vagal sensory neurons via activation of K_{ATP} channels

Whole-cell current clamp recordings revealed that extracellular superfusion of ghrelin (30 nM, saturating concentration) hyperpolarized 19 of 59 (32%) recorded neurons from −56 ± 3 mV to −62 ± 3 mV (Fig. 1*A*). Of the 59 recorded neurons, 19 and 15 were identified projecting to duodenum and lungs, respectively, using the DiI retrograde labelling technique. Nine of 19 (47%) duodenum-projecting neurons and two of 22 (9%) of lung-projecting neurons responded to 30 nM ghrelin. Therefore, it appears that upper gut-projecting nodose ganglia neurons are much more sensitive to ghrelin than those projecting to the lung. The hyperpolarization was associated with a decrease in neuronal input resistance from 320 ± 9 to 281 ± 28 MΩ (78% of control, $n = 8$, $P < 0.01$), a reduction in the number of action potentials at double the strength of the rheobase from 5.5 ± 2.5 to 2.1 ± 1 (35% of control, $P < 0.001$) and an increase in action potential threshold (Fig. 1*A*–*C*). These changes indicate that ghrelin decreased the nodose ganglia excitability.

Analysis of current–voltage relationships before and after ghrelin application revealed that the curves crossed at −105 mV, which is close to the K^+ ion reversal potential under the conditions recorded (Fig. 1*D*). These findings suggest that the actions of ghrelin are mediated by the opening of K^+ channels.

Recent studies from our laboratory indicate that the vagal K_{ATP} channels play an important role in metabolic sensing (Grabauskas *et al.* 2010; Grabauskas *et al.* 2013). We examined whether K_{ATP} channels mediate ghrelin-generated outward currents. Extracellular application of tolbutamide (200 μM), a K_{ATP} channel inhibitor, reversed ghrelin currents ($n = 5$) (Fig. 2*A*). Moreover, concurrent application of tolbutamide and ghrelin blocked the ghrelin currents by 89% (4.5 ± 3 mV, $n = 9$, $P < 0.001$) (Fig. 2*B*).

To confirm the involvement of K_{ATP} channels, we silenced the Kir6.2 subunit using siRNA (Grabauskas *et al.* 2010; Grabauskas *et al.* 2013). The Kir6.2 siRNA was tagged with a Cy3 fluorescent label, which permitted identification of the transfected neurons (Fig. 2*C*, inset). After incubation for 72–96 h, we examined the responsiveness of Cy3-positive vagal neurons to the extracellular application of ghrelin (30 nM). The transfected neurons ($n = 30$) did not respond to either ghrelin (30 nM) or tolbutamide (200 μM) (Fig. 2*C*).

We performed immunohistochemical staining of the vagal nodose ganglia to demonstrate that GHS-R1a colocalizes with the Kir6.2 channel subunit. Our studies showed intense staining of Kir6.2 and GHS-R1a in 72% and 40% of nodose neurons, respectively (Fig. 2*D*–*G*). Among the GHS-R1a-positive neurons, 97% expressed Kir6.2. Thus, the electrophysiological and immunocytochemistry data support the premise that the inhibitory actions of ghrelin are mediated by the opening of K_{ATP} channels, resulting in membrane potential hyperpolarization.

Ghrelin inhibits inward currents generated by leptin and CCK

We performed whole-cell voltage clamp studies to examine the interaction between ghrelin and leptin and also between ghrelin and CCK. We showed that ghrelin (30 nM)

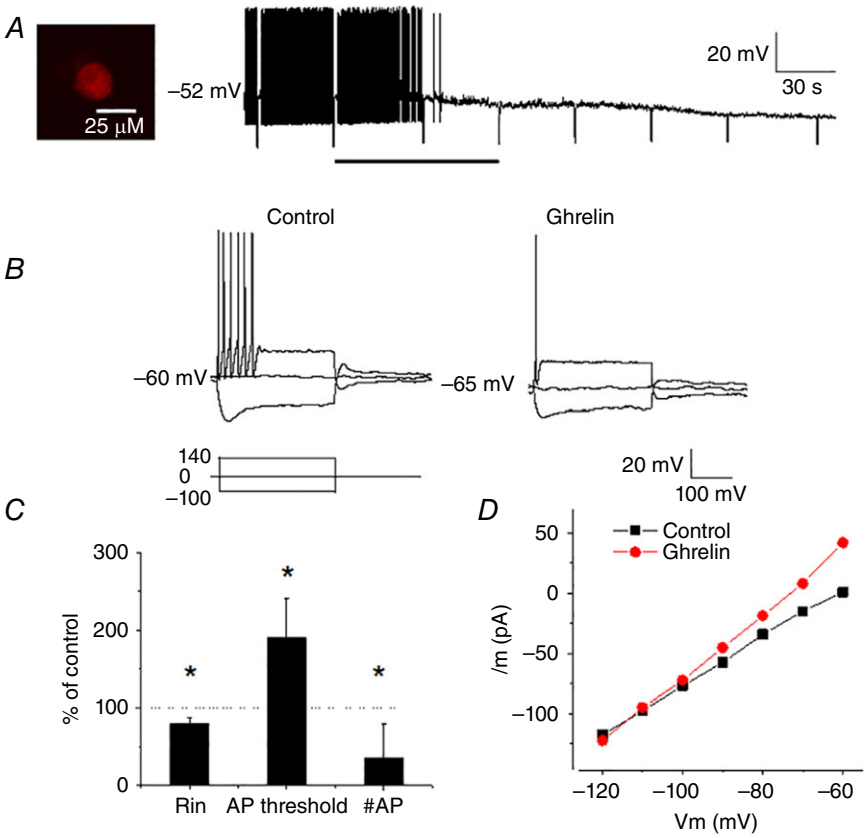

Figure 1. Ghrelin inhibits vagal sensory neurons
A, continuous membrane potential recording from duodenum-projecting neuron (DiI labelled, inset) showing that ghrelin (30 nM; bar) hyperpolarized the membrane potential and reduced the neuronal input resistance. Negative membrane potential deflections display the neuron potential in response to DC current pulses (−100 pA, 500 ms). *B*, current responses showing that extracellular application of ghrelin (30 nM) hyperpolarized the recorded neuron. This hyperpolarization was associated with a decrease in neuronal input resistance, as well as a decrease in the number of action potentials evoked by a DC current pulse of amplitude 140 pA (double rheobase) from 6 to 1. *C*, ghrelin modulates vagal sensory neuron excitability by reducing the neuronal input resistance (Rin), increasing the threshold for action potential initiation and reducing the number of action potentials evoked by a current pulse of the amplitude of double rheobase ($n = 8$, values are the mean ± SEM, $^*P < 0.05$ compared to controls). *D*, current–voltage relationships acquired under control conditions and during ghrelin application showing that the effect reversed at approximately −105 mV, close to the estimated K^+ equilibrium potential under the conditions recorded.

and leptin (10 nM) generated outward and inward currents of maximal amplitude of 44 ± 5 pA (n = 5) and 38 ± 6 pA (n = 5), respectively (Fig. 3*A*). Application of leptin following ghrelin resulted in no significant deviation from the baseline current (5.1 ± 8 pA, Fig. 3*A*, lower).

In a separate series of experiments, we examined the interaction between ghrelin and CCK. Superfusion of CCK-8 (30 nM) generated an inward current of 88 ± 11 pA. Repeated superfusion of CCK-8 in the presence of ghrelin (30 nM) generated an inward current of 40 ± 8 pA (n = 5) (Fig. 3*B*). Analysis of leptin- and CCK-8-generated currents, either alone or in the presence of ghrelin, showed that the resulting currents are the sum of ghrelin and leptin/CCK-8-evoked currents (Fig. 3*C*). Our findings suggest that these currents operate via independent ion channels.

Signal transduction pathways used by ghrelin to activate K_{ATP} channels in the nodose ganglia

Protein phosphorylation plays an important role in the modulation of neuronal excitability. Previous studies identified specific sites on the Kir6.2 channel that are substrates for G protein-activated serine/threonine kinases and also showed that activation of these sites contributes to short- and long-term regulation of current amplitude and kinetics (Béguin *et al.* 1999). We hypothesize that ghrelin stimulates the $G_{\alpha i}$–PI3K–mitogen-activated protein kinase (MAPK)/Erk1/2 pathway to activate the K_{ATP} channels. To test this hypothesis, we examined the effect of ghrelin on PI3K and Erk1/2 expression in cultured rat nodose ganglia neurons. Nodose ganglia neurons were stimulated with 0–100 nM ghrelin for 60 min; PI3K was significantly increased at 3, 10 and 30 nM. The

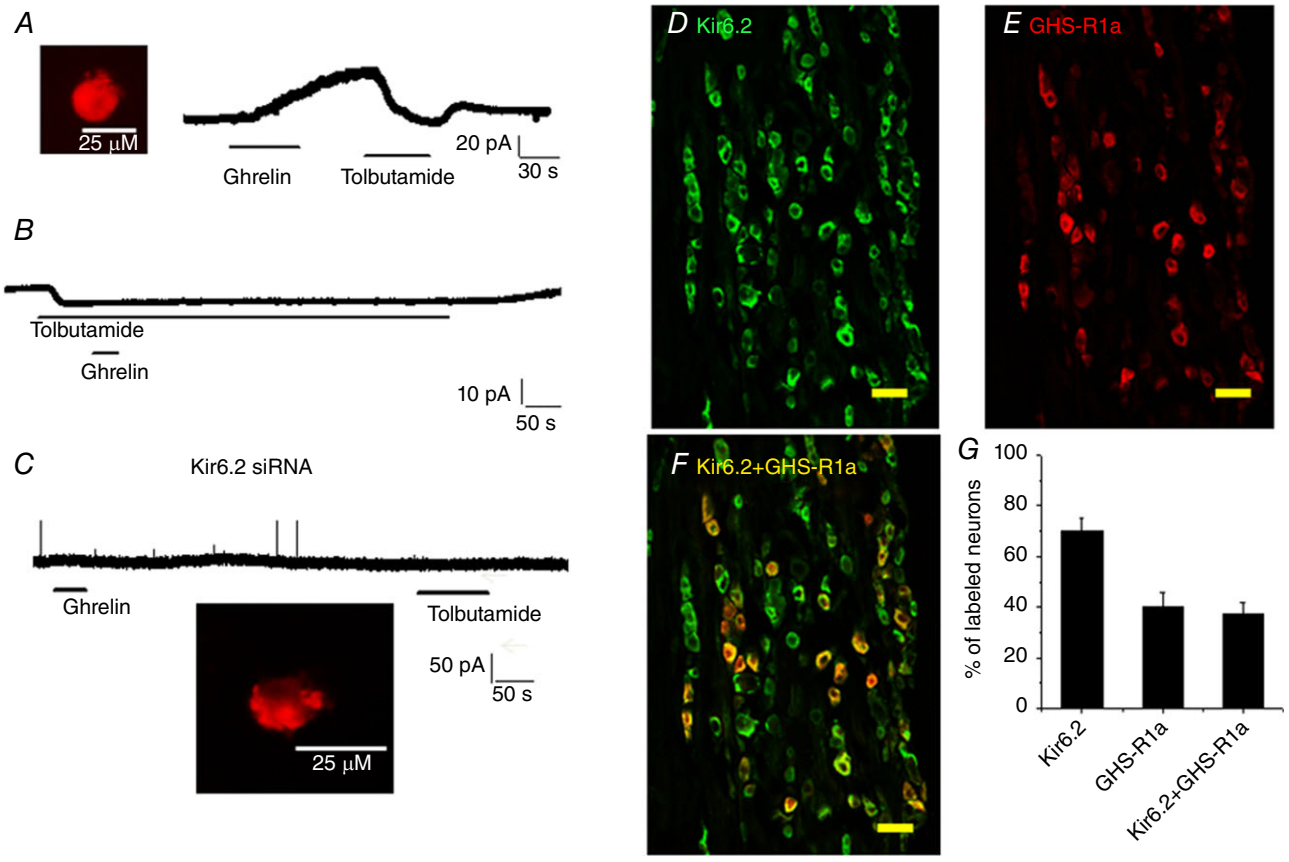

Figure 2. Ghrelin inhibits vagal sensory neurons via activation of K_{ATP} channel
A, continuous current recording showing that tolbutamide (200 μM), a K_{ATP} channel inhibitor, reversed the current induced by ghrelin (30 nM) in a duodenum-projecting neuron (DiI labelled, inset). *B*, representative continuous current recording showing that extracellular application of tolbutamide (200 μM) generated an inward current (10 pA). Subsequent application of ghrelin (30 nM) failed to induce an outward current. *C*, silencing the Kir6.2 channel subunit in a vagal sensory neuron using Kir6.2 Cy3-labelled siRNA abolished both ghrelin and tolbutamide currents. The inset shows a Kir6.2 Cy3-siRNA transfected/labelled neuron. *D–F*, photomicrographs showing anti-Kir6.2 (green) and anti-GHS-R1a (*red*) immunoreactivities in vagal ganglia cross-sections. Superimposition of the green and red images showing that most anti-GHS-R1a immunoreactivity colocalizes with anti-Kir6.2 (yellow). Scale bar, 100 μm. *G*, percentage of neurons in vagal ganglia expressing Kir6.2 and GHS-R1a, as well as both Kir6.2 and GHS-R1a. The data are based on counts from five cross-sections.

dose–response curve showed a bimodal distribution with a maximal increase at 10 nM ghrelin (Fig. 4*A*, Fig. S1*A*). Similarly, ghrelin-stimulated Erk1/2 phosphorylation was significant at 10, 20 and 30 nM, with a maximal increase at 30 nM ghrelin compared to control (Fig. 4*B*, Fig. S1*B*).

Examination of the signal transduction cascade with western blot analysis revealed that ghrelin (30 nM)-induced phosphorylation of Erk1/2 was blocked by PTx (1 U ml^{-1}), a $G_{\alpha i}$ protein inhibitor, and wortmannin (100 nM), a PI3K inhibitor (Fig. 4*C*, Fig. S1*C*). By contrast, U73122 (10 μM), a PLC inhibitor; calphostin C (1 μM), a PKC inhibitor; SQ 22536 (100 μM), an adenylate cyclase inhibitor; and H7 (30 μM), a protein kinase A (PKA) inhibitor, did not block ghrelin-induced Erk1/2 phosphorylation (Fig. 4*C*, Fig. S1*C*). To confirm the involvement of PI3K in cells transfected with PI3K siRNA, ghrelin-stimulated Erk1/2 expression was significantly inhibited (> 90%, $n = 6$) (Fig. 4*D*, Fig. S1*D*). Western blotting showed that transfection with PI3K siRNA caused a 76 ± 4% reduction in PI3K expression.

To confirm that ghrelin acts via the $G_{\alpha i}$–PI3K–MAPK/Erk1/2 pathway to modulate nodose ganglia excitability, we performed whole-cell current clamp recordings. Compared to controls (Fig. 5*A*), neurons dialysed with PTx (1 μ ml^{-1}, $n = 12$, $P < 0.05$) (Fig. 5*B*) showed no response to ghrelin (30 nM). Similarly, transfection with PI3K siRNA ($n = 8$, $P < 0.05$) (Fig. 5*C*) or Erk1/2 siRNA ($n = 8$, $P < 0.05$) (Fig. 5*D*) also abolished ghrelin currents. These results are summarized in a histogram (Fig. 5*E*). Thus, protein expression studies and electrophysiological recordings indicate that ghrelin inhibits vagal sensory neurons via the $G_{\alpha i}$–PI3K–Erk1/2 pathway.

Silencing PI3K, Erk1/2 and K_{ATP} abolishes the inhibitory actions of ghrelin on leptin- and CCK-stimulated nodose neuronal activities *in vivo*

In vivo single-unit discharges of vagal primary afferent neurons innervating the gastrointestinal tract were recorded from rat nodose ganglia as described previously (Li *et al.* 1999). Data were collected from 84 recordings of single nodose ganglia neurons in 18 rats. Under basal conditions, all units were either silent or displayed very low spontaneous activities (0–5 spikes per 20 s bin). All 84 units were activated by electrical stimulation of the subdiaphragmatic vagus nerve. Ghrelin (30 μg kg^{-1} I.V.) did not affect the basal firing rates. However, it markedly reduced nodose neuron firing stimulated by leptin and CCK-8 (Fig. 6). As shown in Fig. 6*A*, the infusion of leptin (225 μg kg^{-1} I.V.) caused the neuronal firing rates to increase from a basal of 0 ± 1 to 14 ± 5 spikes per 20 s ($n = 6$, $P < 0.05$). Similarly, administration of CCK-8 (30 μg kg^{-1}) also increased the firing rate to 23.5 ± 3.5 spikes per 20 s ($n = 5$, $P < 0.05$)(Figs 6*B* and 7*A*). However, when leptin or CCK-8 were administered 30 s after ghrelin injection, the increased firing rates were reduced to 5.1 ± 3 and 9 ± 2.3 spikes per 20 s, respectively ($n = 5$–6, $P < 0.05$)(Fig. 6*A* and *B*).

We genetically silenced the Kir6.2 channel subunit by electroporation of the right nodose ganglia with random (control) or specific Kir6.2 siRNA. RT-PCR data demonstrated that, 5 days after electroporation of the nodose ganglia with Kir6.2 siRNA, Kir6.2 mRNA was reduced by 75% ($n = 3$) (Fig. 6*C*). To ensure that neuronal discharges were recorded from Kir6.2-silenced and GHS-R1a-expressing neurons, the recorded neurons were labelled with neurobiotin after the electrophysiological

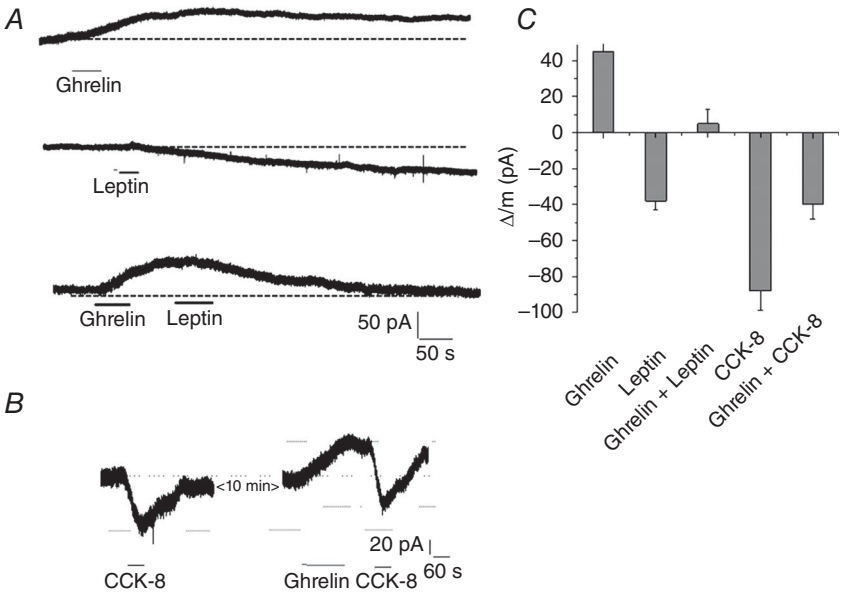

Figure 3. Ghrelin and leptin or CCK-8 activate different antagonistic currents
A, representative current recording in response to ghrelin (30 nM, upper trace), leptin (10 nM, middle trace), and ghrelin and leptin combined (lower trace). Note that ghrelin generated an outward current (upper trace) that was slowly decaying. However, when ghrelin was paired with leptin, the outward current was reversed. *B*, representative current recording in response to CCK-8 (30 nM) and, 10 min later, in response to ghrelin (30 nM) and CCK-8 (30 nM). Note that the second application of CCK-8 generated a current that was similar in amplitude but 'displaced' by the ghrelin-generated current. The shift from the baseline generated by the first and second applications of CCK-8 was 78 pA and 42 pA, respectively. *C*, pooled data of maximum current amplitudes generated by ghrelin ($n = 5$), leptin ($n = 5$), CCK-8 ($n = 5$) and ghrelin-leptin/CCK-8 groupings ($n = 5$).

recordings (Fig. 7*A* and 7*B*). Our immunohistochemical data demonstrated that Kir6.2 gene silencing reduced the number of anti-Kir6.2-positive cells from 72% to 15% ($n = 5$). Only neurons that showed no immunoreactivity to anti-Kir6.2 but were immunoreactive to anti-GHS-R1a were included in our data analysis (Fig. 7*B*). As shown in Fig. 6*A*, *B* and *D*, after silencing Kir6.2, ghrelin failed to inhibit leptin- ($n = 6$) and CCK-8- ($n = 6$) evoked neuronal firing.

In separate studies, we showed that silencing the gene expression of Erk1/2 or PI3K in the nodose ganglia by electroporation of specific siRNAs also abolished the inhibitory actions of ghrelin (30 μg kg^{-1} I.V.) on leptin- ($n = 6$) and CCK-8- ($n = 6$) induced responses (Fig. 6*E* and *F*). RT-PCR data demonstrated that, 5 days after electroporation of Erk1/2 siRNA and PI3K siRNA, the gene expression of Erk1/2 and PI3K was reduced > 80%.

Silencing Kir6.2 in the nodose ganglia abolishes the orexigenic actions of ghrelin on feeding

To provide direct evidence that the K_{ATP} channel in the nodose ganglia mediates the orexigenic actions of ghrelin, we performed feeding studies in three groups of rats after a 12 h fast: (i) control rats treated with I.P. saline; (ii) control rats treated with ghrelin (30 μg kg^{-1} I.P., 30 min before feeding); and (iii) rats 5 days after silencing of Kir6.2

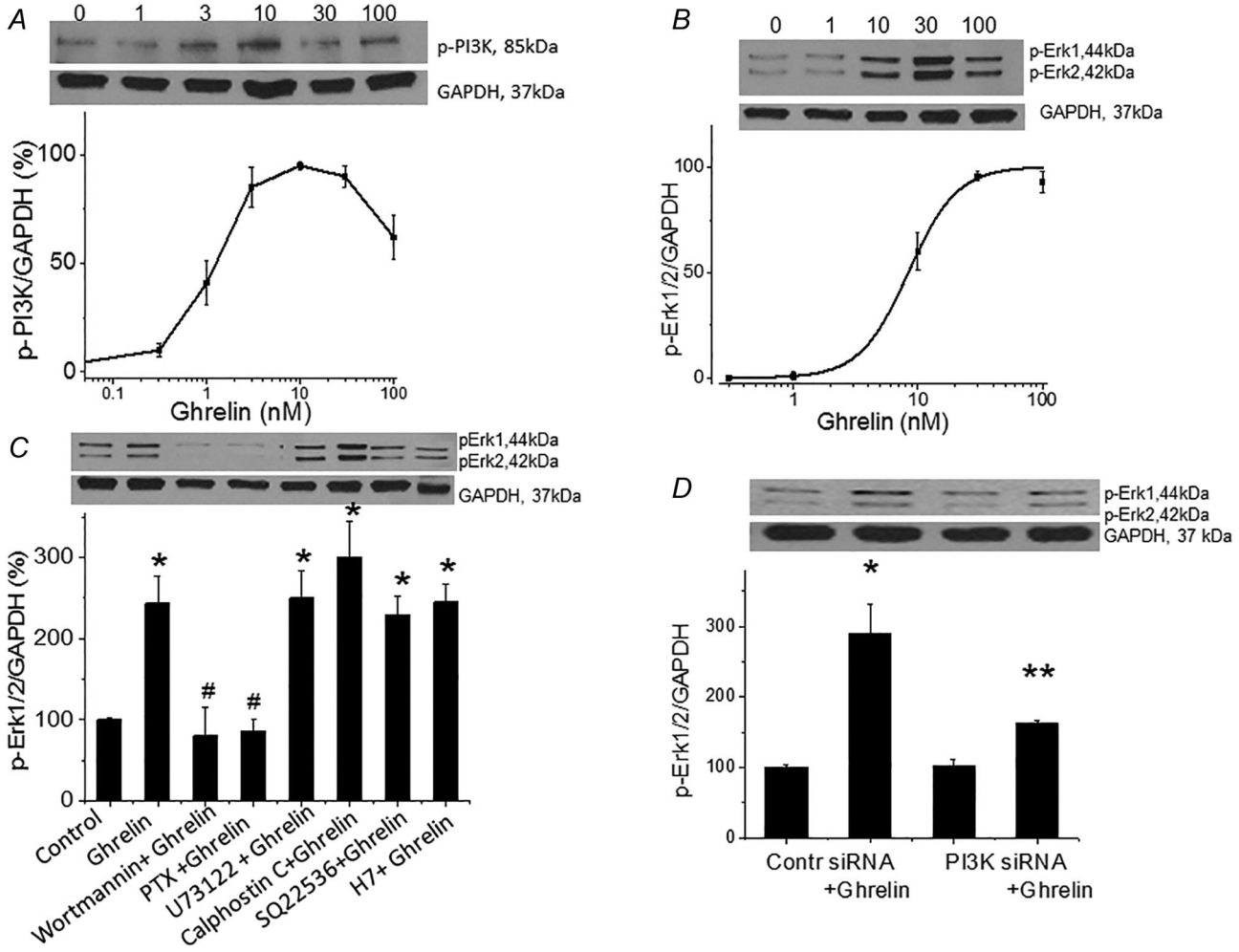

Figure 4. Ghrelin stimulates p-PI3K and p-Erk1/2 in the nodose ganglia
A, western blot showing that ghrelin stimulates nodose ganglia p-PI3K in a dose-dependent manner ($n = 6$). *B*, western blot showing that ghrelin stimulates nodose ganglia p-Erk1/2 in a dose-dependent manner ($n = 6$). *C*, ghrelin (20 nM)-stimulated p-Erk1/2 was inhibited by wortmannin (100 mM) and PTx (1 U ml^{-1}) but not by PLC inhibitor U73122 (10 μM), PKC inhibitor calphostin C (1 μM), adenylate cyclase SQ 22536 (100 μM) or PKA inhibitor H7 (30 μM) in the nodose ganglia ($n = 5$–6, $^{*}P < 0.05$ compared to basal controls; $^{\#}P < 0.05$ compared to stimulation by ghrelin). *D*, Western blot showing ghrelin-stimulated Erk1 and Erk2 mRNA expression in vagal ganglia 96 h after transfection with random siRNA but not with PI3K siRNA [$n = 4$, $^{*}P < 0.05$ compared to basal control; $^{**}P < 0.05$ compared to nodose ganglia transfected with control (random) siRNA].

in the nodose ganglia and treated with ghrelin (30 μg kg^{-1} I.P., 30 min before feeding). In the control group whose right and left nodose ganglia were electroporated with random siRNA, I.P. injection of ghrelin stimulated food intake in the first, second and third hours of feeding compared to rats treated with I.P. saline ($n = 6$, $P < 0.05$) (Fig. 8*A*). Silencing Kir6.2 expression in both nodose ganglia completely prevented the orexigenic actions of ghrelin during the first 3 h of feeding (n = 6, $P < 0.05$) (Fig. 8*A*). Indeed, the accumulative food intake in the first, second, and third hours was less compared to that in the control group, which was not treated with ghrelin. This suggests that the K_{ATP} channel in the nodose ganglia also mediates the orexigenic actions of endogenous ghrelin.

Discussion

We have shown for the first time that ghrelin modulates the excitability of the nodose ganglia by activating a K_{ATP} conductance. We provide substantive experimental evidence to support this conclusion: (1) immunocytochemistry studies showed that almost all GSH-R1a-containing neurons in the nodose ganglia expressed K_{ATP} channels; (ii) analysis of current–voltage relationships for the ghrelin-induced current exhibited a negative slope conductance that reversed at approximately −105 mV, which is consistent with activation of K^+ ion channels under the recording conditions; (iii) application of the K_{ATP} antagonist tolbutamide abolished ghrelin-induced currents, as shown by our patch clamp studies; (d) *in vitro* and *in vivo* studies demonstrated that the inhibitory actions of ghrelin were abolished in rat vagal sensory neurons transfected with Kir6.2 siRNA; and (e) silencing Kir6.2 in vagal sensory neurons abolished the orexigenic actions of ghrelin on food intake. These findings indicate that ghrelin inhibits vagal sensory neurons via activation of K_{ATP} channels. In addition, our patch clamp recordings and protein expression studies showed that the $G_{\alpha i}$–PI3K–Erk1/2–K_{ATP} signalling cascade mediates the actions of ghrelin (Fig. 8*B*). The resulting hyperpolarization rendered the nodose ganglia less responsive to signals evoked by anorexigenic hormones.

ATP-sensitive K^+ channels couple cell metabolism to electrical activity in a variety of cell types by regulating K^+ fluxes across the cell membrane. Heightened metabolism leads to channel closure, membrane depolarization and electrical firing. Reduced metabolism, in contrast, opens K_{ATP} channels and decreases electrical activity. In endocrine cells, K_{ATP} channels play a critical role in the release of hormones, such as insulin from pancreatic β cells (Ashcroft *et al.* 1984) and glucagon from pancreatic α cells (Göpel *et al.* 2000). In the CNS, K_{ATP} channels modulate electrical activity and neurotransmitter release (Amoroso *et al.* 1990; Avshalumov & Rice, 2003), whereas, in the heart, K_{ATP} channels mediate cardioprotection against

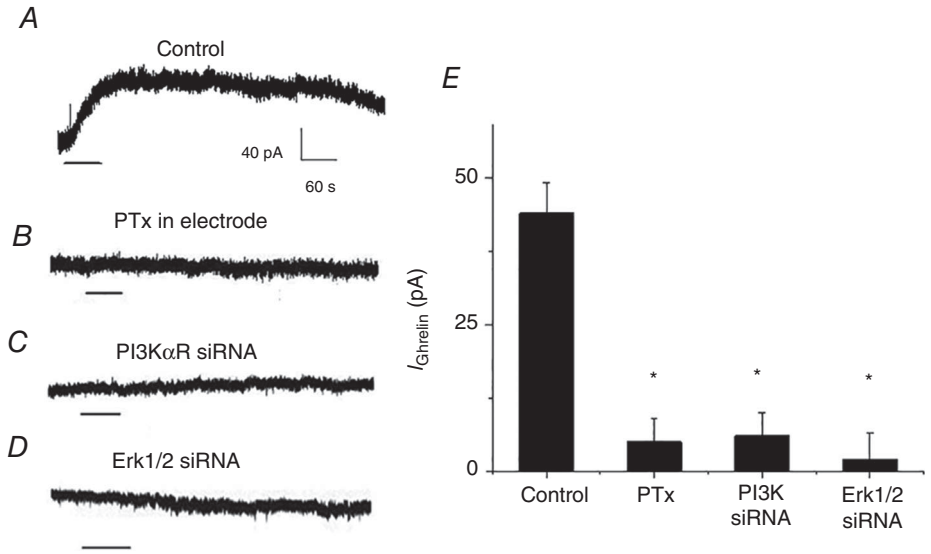

Figure 5. Electrophysiological evidence that $G_{\alpha i}$, PI3K and Erk1/2 mediate the actions of ghrelin in the nodose ganglia
A, representative current recording showing that extracellular application of ghrelin (30 nM) generated an outward current ($n = 12$). *B*, representative current recording showing that inclusion of PTx (1 U ml^{-1}) in the recording electrode media abolished ghrelin-induced currents ($n = 9$). *C*, representative current recording showing that ghrelin-induced currents were abolished in PI3K siRNA-transfected neurons ($n = 10$). *D*, representative current recording showing that ghrelin-induced currents were abolished in Erk1 and Erk2 siRNA-transfected neurons ($n = 12$). *E*, ghrelin currents ($n = 12$) were inhibited by PTx ($n = 9$) and by transfection of nodose ganglia neurons with PI3K siRNA ($n = 10$) or Erk1 and Erk2 siRNA ($n = 12$). *$P < 0.05$ compared to ghrelin-treated neurons.

ischaemia/reperfusion injury (Suzuki *et al.* 2002). In the present study, we show that K_{ATP} channels mediate the inhibitory actions of ghrelin on vagal sensory neurons and we propose a mechanism to explain the actions of ghrelin with respect to overcoming anorexigenic signals from different origins. Plasma ghrelin levels in rats are reported to increase during prolonged fasting when energy metabolism is low (Li *et al.* 2009). We show that ghrelin opens K_{ATP} channels and reduces vagal sensory neuronal firing so that the nodose ganglia become less responsive to stimulation by anorexigenic signals, such as CCK and leptin. We have shown that, on feeding, nodose

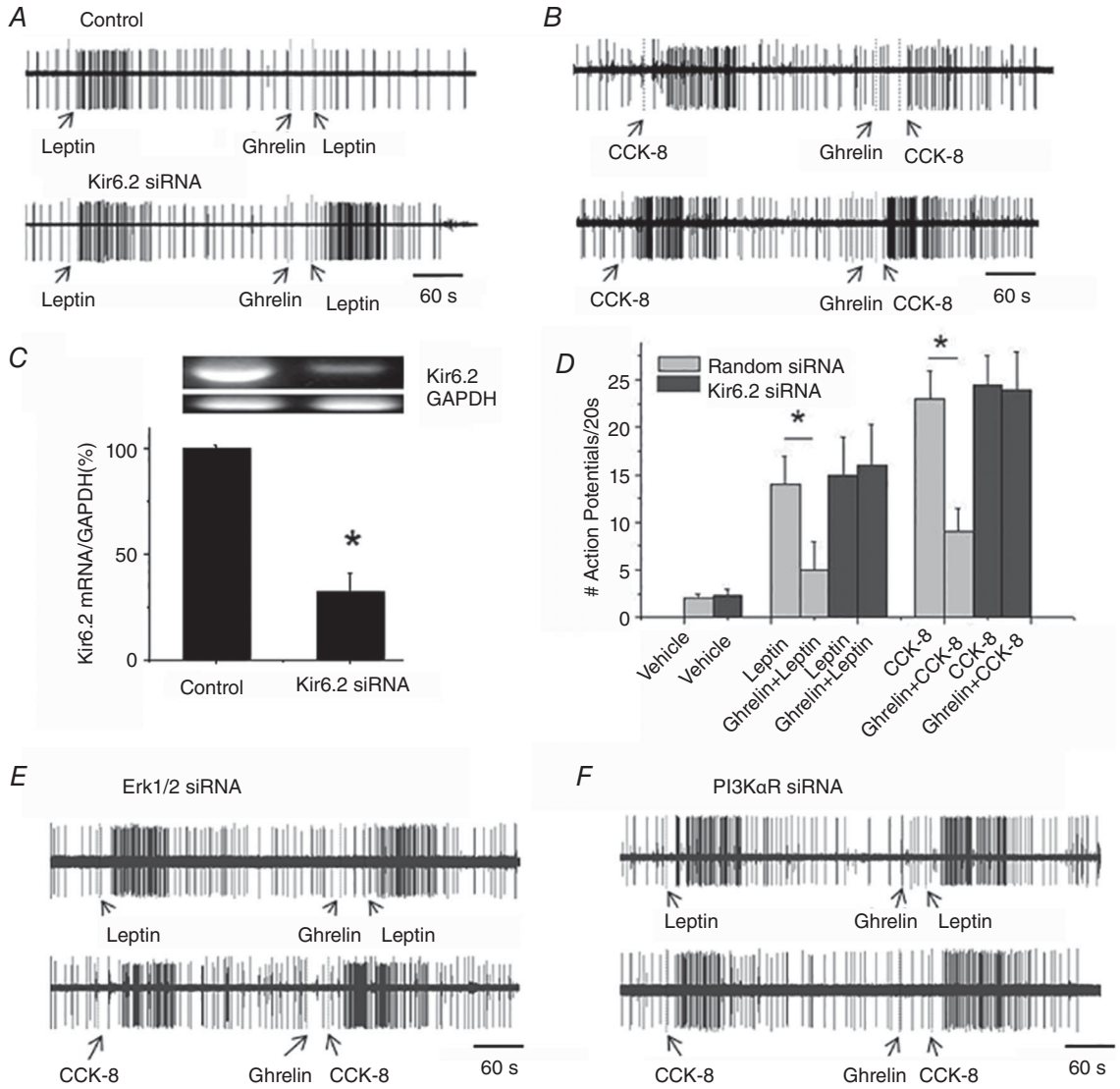

Figure 6. Kir6.2 subunit mediates the inhibitory actions of ghrelin inhibition *in vivo*
A, single-unit recordings in response to leptin (225 μg kg^{-1} I.V.) and leptin after ghrelin administration (25 μg kg^{-1} I.V.) from the right nodose ganglia, which were electroporated with Kir6.2 channel siRNA (lower trace). *B*, single-unit recordings in response to CCK-8 (30 μg kg^{-1} I.V.) and CCK-8 after ghrelin administration (25 μg kg^{-1} I.V.) in the right nodose ganglia, which were electroporated with Kir6.2 channel siRNA (lower trace). *C*, Kir6.2 mRNA expression (RT-PCR) in vagal ganglia 96 h after electroporation with control (random) siRNA and Kir6.2 siRNA ($n = 4$, $^*P < 0.05$ compared to control). *D*, discharges of vagal sensory neurons in response to I.V. injections of leptin and CCK-8 were inhibited by ghrelin in control siRNA-treated animals. The inhibitory actions of ghrelin were abolished in rats whose right nodose ganglia were electroporated with Kir6.2 siRNA ($n = 5$–6, $^*P < 0.05$ compared to control). *E*, single-unit discharge in response to leptin (225 μg kg^{-1} I.V.) and leptin after the administration of ghrelin (25 μg kg^{-1} I.V.) (upper) or CCK-8 (30 μg kg^{-1} I.V.) and CCK-8 after the administration of ghrelin (25 μg kg^{-1} I.V.) (lower) in the right nodose ganglia, which were electroporated with Erk1/2 siRNA. *F*, single-unit discharge in response to leptin (225 μg kg^{-1} I.V.) and leptin after the administration of ghrelin (25 μg kg^{-1} I.V.) in nodose ganglia treated with PI3K siRNA (upper) or CCK-8 (30 μg kg^{-1} I.V.) and CCK-8 after the administration of ghrelin (25 μg kg^{-1} I.V.) in the right nodose ganglia, which were electroporated with Erk1/2 siRNA.

ganglia neurons sense the blood glucose concentration by increasing firing frequency through inactivation of K_{ATP} channels (Grabauskas *et al.* 2010; Grabauskas *et al.* 2013). In this manner, K_{ATP} channels in the nodose ganglia couple metabolism to electrical activity to regulate feeding behaviour.

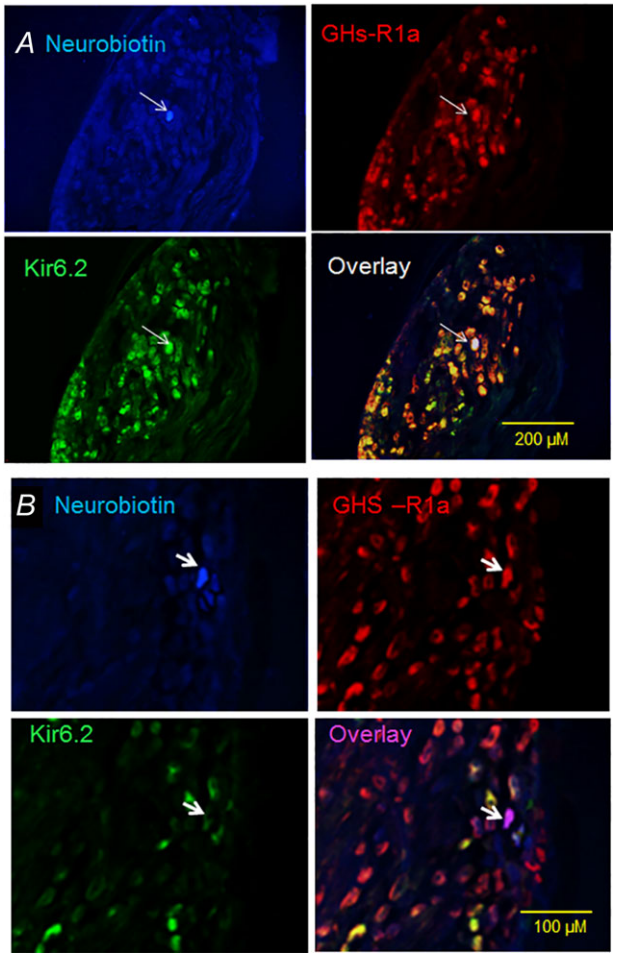

Figure 7. Immunostaining of rat nodose ganglia showing neurons targeted for electrophysiological recording
A, photomicrographs of vagal ganglia cross-sections showing a neuron (arrow) injected with neurobiotin (blue) after electrophysiological recording. This neuron expresses both anti-Kir6.2 (green) and anti-GHS-R1a (red) immunoreactivities. Superimposition of the green and red images (overlay) showing that most of the anti-GHS-R1a immunoreactivity colocalizes with anti-Kir6.2 (yellow). Note that the recorded neuron labelled with neurobiotin contains Kir6.2 and GHS-R1a immunoreactivities (white). *B*, photomicrographs showing a neuron (arrow) injected with neurobiotin (blue) after electrophysiological recording in a Kir6.2 siRNA-electroporated animal. This neuron exhibits strong immunoreactivity to anti-GHS-R1a (red) but little immunoreactivity to anti-Kir6.2 (green). Note that few neurons in the overlay image coexpress Kir6.2 and GHS-R1a (yellow). The recorded neuron (arrow in overlay image) shows no immunoreactivity to Kir6.2 but expresses GHS-R1a (purple).

The classic mechanism by which G protein-coupled receptors activate Erk1/2 is through the heterotrimeric G proteins. Ghrelin has been shown to activate multiple signal transduction pathways in different tissues (Maccarinelli *et al.* 2005; Duxbury *et al.* 2003; Camiña *et al.* 2007; Mousseaux *et al.* 2006). In human aortic smooth muscle cells, ghrelin activates the adenylate cyclase–cAMP–PKA signalling pathway to inhibit muscle contraction and proliferation (Rossi *et al.* 2009). Ghrelin may stimulate angiogenesis via the PI3K/Akt-activated mitogen-activated protein kinase kinase/Erk pathways in rat cardiac microvascular endothelial cells (Wang *et al.* 2012). In the nigrostriatal system, ghrelin stimulates the PLC–PKC cascades, which results in inhibition of

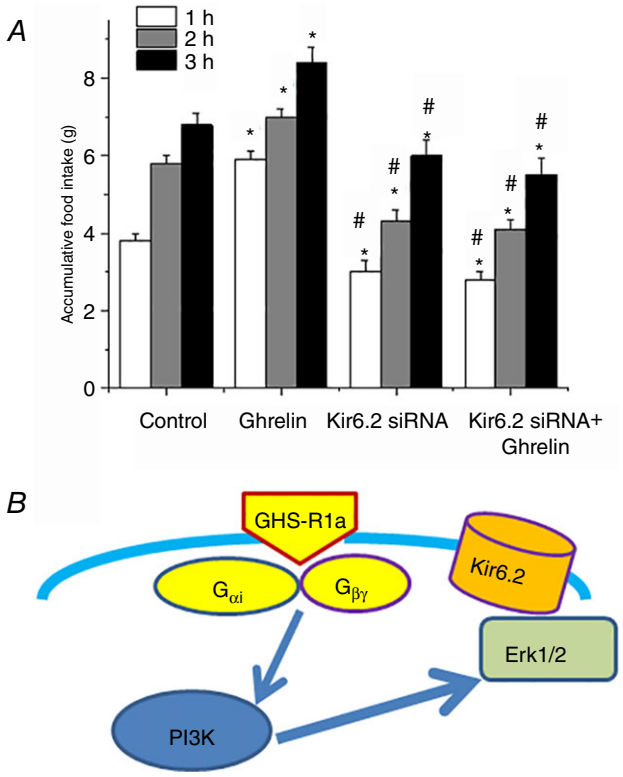

Figure 8. Silencing the Kir6.2 channel in vagal sensory ganglia abolishes the stimulating effect of ghrelin on food intake
A, effect of I.P. injection of ghrelin (25 μg kg^{-1}) or saline on cumulative food intake in rats whose vagal sensory ganglia were bilaterally electroporated with random siRNA (control and ghrelin groups) and Kir6.2 siRNA. $^{*}P < 0.05$ compared to the saline group whose nodose ganglia were treated with random siRNA control. $^{\#}P < 0.05$ compared to the ghrelin-treated group whose nodose ganglia were treated with random siRNA ($n = 4$ in each group). *B*, schematic showing ghrelin signalling and K_{ATP}/Kir6.2 activation in vagal sensory ganglia neurons. These findings suggest that ghrelin binds to its receptor GHS-R1a in the nodose ganglia neuron to dissociate $G_{\alpha i}$ and $G_{\beta\gamma}$, which activates PI3K. PI3K, in turn, stimulates Erk1/2 to phosphorylate the Kir6.2 channel subunit, leading to the opening of K_{ATP} channels and hyperpolarization of the neurons. These events inhibit vagal neuron excitability.

Kv7/KCNQ channels (Shi *et al.* 2013). In the nodose ganglia, we show that ghrelin-induced phosphorylation of Erk1/2 was blocked by PTx or wortmannin but not H7 (PKA inhibitor), SQ 22536 (adenylate cyclase inhibitor) or calphostin C (PKC inhibitor). These findings indicate that GHS-R1a in vagal sensory neurons is $G_{\alpha i/o}$ coupled and activates the PI3K–Erk1/2 pathway via mechanisms independent of PKC and/or PKA. To confirm that ghrelin acts via the $G_{\alpha i}$–PI3K–MAPK/Erk1/2 cascade (Hawes *et al.* 1996) (Fig. 8*B*) to modulate nodose ganglia excitability, we show that neurons dialysed with PTx, which selectively binds to and 'disables' $G_{\alpha i/o}$, fail to respond to ghrelin. Furthermore, transfection with PI3K siRNA or Erk1/2 siRNA also abolishes ghrelin currents.

To provide direct evidence that K_{ATP} channels in the nodose ganglia play a critical role in mediating the orexigenic actions of ghrelin, we silenced K_{ATP} gene expression by electroporation of the nodose ganglia with Kir6.2 siRNA and plasmid pEGFP-N1 carrying the GFP gene. Electroporation uses short, high-voltage pulses to overcome the barrier of the cell membrane (Saito, 2006). This transient permeabilization can be used to load cells with drugs, tracers, RNA and DNA. This approach is safe for animals and humans (Saito, 2006). We have successfully applied this technique to introduce siRNA into nodose ganglia cells (Zhou *et al.* 2011) and the anterior gyrus (Fan *et al.* 2009). By silencing K_{ATP} channel expression in the nodose ganglia, without affecting the expression of this gene in other systems, we could specifically examine the role of K_{ATP} channels in the nodose ganglia in the mediation of the orexigenic actions of ghrelin. We confirmed our success in knocking down Kir6.2 gene expression by RT-PCR and immunohistochemistry. In rats whose nodose ganglia were treated with Kir6.2 siRNA to silence the expression of K_{ATP} channels, ghrelin failed to inhibit leptin- and CCK-8-evoked neuronal firing (Fig. 6). Similarly, this group of rats also failed to respond to ghrelin in feeding behaviour studies (Fig. 8*A*).

Accumulating evidence suggests that the vagus plays an important role in the transmission of peripheral satiety and orexigenic signals to the CNS. In addition to receptors for anorexigenic hormones, such as CCK (Zarbin *et al.* 1981) and leptin (Burdyga *et al.* 2002), the vagal sensory neurons also express receptors for orexigenic agents, such as ghrelin (Sakata *et al.* 2003), orexin A (Burdyga *et al.* 2003), cannabinoid (Burdyga *et al.* 2004) and melanin-concentrating hormone (Burdyga *et al.* 2006*b*). The nodose ganglia probably serve as a site of interaction for various peripheral signals involved in peptide regulation. For example, the synergistic interaction between CCK and leptin mediated by PI3K and signal transducer and activator of transcription 3 signalling pathways at the level of the nodose ganglia helps to amplify the satiety signal to control feeding (Heldsinger *et al.* 2011). On the other hand, the orexigenic hormone ghrelin and satiety factors, such as leptin and CCK, act in opposition to regulate feeding. Recently, we showed that ghrelin induces leptin resistance at the level of the nodose ganglia by increasing suppressor of cytokine signalling 3 (SOCS3) expression, which impairs leptin signalling and increases food intake in male rats (Heldsinger *et al.* 2014). However, increased SOCS3 expression probably does not explain the antagonistic actions of ghrelin on the satiety signals evoked by CCK because the actions of CCK are not affected by SOCS3 expression in the nodose ganglia (Heldsinger *et al.* 2014). Other studies have reported that ghrelin may reverse the satiety effects of CCK by decreasing cannabinoid 1 and melanin-concentrating hormone expression in the nodose ganglia (Burdyga *et al.* 2006*a*). These novel mechanisms may explain the antagonistic actions of ghrelin with respect to reducing the satiety actions of individual hormones under specific experimental conditions; however, they do not adequately explain the actions of ghrelin with respect to overcoming a wide range of anorexigenic signals that act by different intracellular mechanisms. Our demonstration that ghrelin induces hyperpolarization of the nodose ganglia via activation of K_{ATP} channels, rendering the nodose less responsive to satiety signals, provides a novel mechanism to explain the ability of ghrelin to overcome satiety signals that act via diverse signal transduction pathways. We observed that ghrelin not only inhibits leptin- and CCK-evoked vagal firing, but also it attenuates satiety signals generated by bombesin and uroguanylin, which act via different signalling cascades (Wu X, Owyang C, unpublished observations). Arnold *et al.* (2006) reported that subdiaphragmatic vagal deafferentation did not abolish eating induced by I.P. injection of ghrelin. However, this does not rule out the possibility that ghrelin acts on the vagal pathway to modulate satiety because our data showed that ghrelin can act directly on the soma of the nodose ganglia neurons.

Our observations may have pathophysiological significance. In healthy subjects, plasma ghrelin levels increase during overnight fasting and decline 30 min postprandially. In obese subjects, food fails to suppress ghrelin levels (English *et al.* 2002). On the other hand, malfunctioning of the intracellular signal cascades to activate K_{ATP} channels in the nodose ganglia may contribute to the pathophysiology of early satiety and eating disorders.

In conclusion, using a multilayered approach that includes immunocytochemistry, western blotting, patch clamp electrophysiology studies and gene silencing techniques in cultured rat nodose ganglia neurons, as well as *in vivo* single-cell electrical recordings and feeding studies, we show that ghrelin modulates the excitability of the nodose ganglia by activating a K_{ATP} conductance. The resulting hyperpolarization renders the neurons less

responsive to signals evoked by anorexigenic hormones. This provides a mechanism to explain the actions of ghrelin with respect to overcoming anorexigenic signals that act via the vagal afferent pathways and stimulate feeding.

References

Amoroso S, Schmid-Antomarchi H, Fosset M & Lazdunski M (1990). Glucose, sulfonylureas, and neurotransmitter release: role of ATP-sensitive K^+ channels. *Science* **247**, 852–854.

Arnold M, Mura A, Langhans W & Geary N (2006). Gut vagal afferents are not necessary for the eating-stimulatory effect of intraperitonially injected ghrelin in the rat. *J Neurosci* **26**, 11052–11060.

Ashcroft FM, Harrison DE & Ashcroft SJ (1984). Glucose induces closure of single potassium channels in isolated rat pancreatic beta-cells. *Nature* **312**, 446–448.

Au CM, Luk SK, Jackson CJ, Ng HK, Yow CM & To SS (2006). Differential effects of photofrin, 5-aminolevulinic acid and calphostin C on glioma cells. *J Photochem Photobiol B* **85**, 92–101.

Avshalumov MV & Rice ME (2003). Activation of ATP-sensitive K^+ (K_{ATP}) channels by H_2O_2 underlies glutamate-dependent inhibition of striatal dopamine release. *Proc Natl Acad Sci U S A* **100**, 11729–11734.

Barbieri JT & Cortina G (1988). ADP-ribosyltransferase mutations in the catalytic S-1 subunit of pertussis toxin. *Infect Immun.* **56**, 1934–1941.

Barrachina MD, Martinez V, Wang L, Wei JY & Taché Y (1997). Synergistic interaction between leptin and cholecystokinin to reduce short-term food intake in lean mice. *Proc Natl Acad Sci U S A* **94**, 10455–10460.

Béguin P, Nagashima K, Nishimura M, Gonoi T & Seino S (1999). PKA-mediated phosphorylation of the human K (ATP) channel: separate roles of Kir6.2 and SUR1 subunit phosphorylation. *EMBO J* **18**, 4722–4732.

Browning KN (2013). Modulation of gastrointestinal vagal neurocircuits by hyperglycemia. *Front Neurosci* **7**, 217.

Burdyga G, Spiller D, Morris R, Lal S, Thompson DG, Saeed S, Dimaline R, Varro A & Dockray GJ (2002). Expression of the leptin receptor in rat and human nodose ganglion neurons. *Neuroscience* **109**, 339–347.

Burdyga G, Lal S, Spiller D, Jiang W, Thompson D, Attwood S, Saeed S, Grundy D, Varro A, Dimaline R & Dockray GJ (2003). Localization of orexin-1 receptors to vagal afferent neurons in the rat and humans. *Gastroenterology* **124**, 129–139.

Burdyga G, Lal S, Varro A, Dimaline R, Thompson DG & Dockray GJ (2004). Expression of cannabinoid CB1 receptors by vagal afferent neurons is inhibited by cholecystokinin. *J Neurosci* **24**, 2708–2715.

Burdyga G, Varro A, Dimaline R, Thompson DG & Dockray DJ (2006*a*). Feeding-dependent depression of melanin-concentrating hormone and melanin-concentrating hormone receptor-1 expression in vagal afferent neurons. *Neuroscience* **137**, 1405–1415.

Burdyga G, Varro A, Dimaline R, Thompson DG & Dockray GJ (2006*b*). Ghrelin receptors in rat and human nodose ganglia: putative role in regulating CB-1 and MCH receptor abundance. *Am J Physiol Gastrointest Liver Physiol* **290**, G1289–G1297.

Camiña JP, Lodeiro M, Ischenko O, Martini AC & Casanueva FF (2007). Stimulation by ghrelin of p42/p44 mitogen-activated protein kinase through the GHS-R1a receptor: role of G-proteins and beta-arrestins. *J Cell Physiol* **213**, 187–200.

Cui RJ, Li X & Appleyard SM (2011). Ghrelin inhibits visceral afferent activation of catecholamine neurons in the solitary tract nucleus. *J Neurosci* **31**, 3484–3492.

Date Y, Murakami N, Toshinai K, Matsukura S, Niijima A, Matsuo H, Kangawa K & Nakazato M (2002). The role of the gastric afferent vagal nerve in ghrelin-induced feeding and growth hormone secretion in rats. *Gastroenterology* **123**, 1120–1128.

Date Y, Toshinai K, Koda S, Miyazato M, Shimbara T, Tsuruta T, Niijima A, Kangawa K & Nakazato M (2005). Peripheral interaction of ghrelin with cholecystokinin on feeding regulation. *Endocrinology* **146**, 3518–3525.

De Lartigue G, Barbier de la Serre C, Espero E, Lee J & Raybould HE (2012). Leptin resistance in vagal afferent neurons inhibits cholecystokinin signaling and satiation in diet induced obese rats. *PLoS ONE* **7**, e32967.

Dickson SL & Luckman SM (1997). Induction of c-fos messenger ribonucleic acid in neuropeptide Y and growth hormone (GH)-releasing factor neurons in the rat arcuate nucleus following systemic injection of the GH secretagogue, GH-releasing peptide-6. *Endocrinology* **138**, 771–777.

Duxbury MS, Waseem T, Ito H, Robinson MK, Zinner MJ, Ashley SW & Whang EE (2003). Ghrelin promotes pancreatic adenocarcinoma cellular proliferation and invasiveness. *Biochem Biophys Res Comm* **309**, 464–468.

English PJ, Ghatei MA, Malik IA, Bloom SR & Wilding JP (2002). Food fails to suppress ghrelin levels in obese humans. *J Clin Endocrinol Metab* **87**, 2984–2987.

Fan J, Wu X, Cao Z, Chen S, Owyang C & Li Y (2009). Up-regulation of anterior cingulate cortex NR2B receptors contributes to visceral pain responses in rats. *Gastroenterology* **136**, 1732–1740.

Gao J, Wu X, Owyang C & Li Y (2006). Enhanced responses of the anterior cingulate cortex neurons to colonic distension in viscerally hypersensitive rats. *J Physiol* **570**, 169–183.

Gnanapavan S, Kola B, Bustin SA, Morris DG, McGee P, Fairclough P, Bhattacharya S, Carpenter R, Grossman AB & Korbonits M (2002). The tissue distribution of the mRNA of ghrelin and subtypes of its receptor, GHS-R, in humans. *J Clin Endocrinol Metab* **87**, 2988.

Göpel SO, Kanno T, Barg S, Weng XG, Gromada J & Rorsman P (2000). Regulation of glucagon release in mouse-cells by the K_{ATP} channels and inactivation of TTX-sensitive NA^+ channels. *J Physiol* **528**, 509–520.

Grabauskas G, Lancaster B, O'Connor V & Wheal HV (2007). Protein kinase signalling requirements for metabotropic action of kainate receptors in rat CA1 pyramidal neurons. *J Physiol* **579**, 363–373.

Grabauskas G, Song I, Zhou S & Owyang C (2010). Electrophysiological identification of glucose-sensing neurons in rat nodose ganglia. *J Physiol* **588**, 617–632.

Grabauskas G, Zhou SY, Lu Y, Song I & Owyang C (2013). Essential elements for glucosensing by gastric vagal afferents: immunocytochemistry and electrophysiology studies in the rat. *Endocrinology* **154**, 296–307.

Hawes BE, Luttrell LM, van Biesen T & Lefkowitz RJ (1996). Phosphatidylinositol 3-kinase is an early intermediate in the G beta gamma-mediated mitogen-activated protein kinase signaling pathway. *J Biol Chem* **271**, 12133–12136.

Heldsinger A, Grabauskas G, Song I & Owyang C (2011). Synergistic interaction between leptin and cholecystokinin in the rat nodose ganglia is mediated by PI3K and STAT3 signaling pathways: implications for leptin as a regulator of short term satiety. *J Biol Chem* **286**, 11707–11715.

Heldsinger A, Lu Y, Zhou SY, Grabauskas G, Song I & Owyang C (2012). Cocaine- and amphetamine-regulated transcript is the neurotransmitter regulating the action of cholecystokinin and leptin on short-term satiety in rats. *Am J Physiol Gastrointest Liv Physiol* **303**, G1042–G1051.

Heldsinger A, Grabauskas G, Wu X, Zhou S, Lu Y, Song I, Owyang C (2014). Ghrelin induces leptin resistance by activation of SOCS3 (suppressor of cytokine signaling 3) expression in male rats: Implications in satiety regulation. *Endocrinology* **155**, 3956–3969.

Kentish S, Li H, Philp LK, O'Donnell TA, Isaacs NJ, Young RL, Wittert GA, Blackshaw LA & Page AJ (2011). Diet-induced adaptation of vagal afferent function. *J Physiol* **590**, 209–221.

Kobashi M, Yanagihara M, Fujita M, Mitoh Y & Matsuo R (2009). Fourth ventricular administration of ghrelin induces relaxation of the proximal stomach in the rat. *Am J Physiol Regul Integr Comp Physiol* **296**, R217–R223.

Kojima M, Hosoda H, Date Y, Nakazato M, Matsuo H & Kangawa K (1999). Ghrelin is a growth-hormone-releasing acylated peptide from stomach. *Nature* **402**, 656–660.

le Roux CW, Neary NM, Halsey TJ, Small CJ, Martinez-Isla AM, Ghatei MA, Theodorou NA & Bloom SR (2005). Ghrelin does not stimulate food intake in patients with surgical procedures involving vagotomy. *J Clin Endocrinol Metab* **90**, 4521–4524.

Levin BE (2001). Glucose sensing neurons do more than just sense glucose. *Int J Obesity* **25**, S68–S72.

Li RY, Li XS, Shao L, Wu ZY, Du WH, Li SX, Zhao SX, Chen KM, Chen MD & Song HD (2009). Influence of visceral adiposity on ghrelin secretion and expression in rats during fasting. *J Mol Endocrinol* **42**, 67–74.

Li Y, Zhu J & Owyang C (1999). Electrical physiological evidence for high and low-affinity vagal CCK-A receptors. *Am J PhysiolGastrointest Liv Physiol* **277**, G469–G477.

Li Y, Wu X, Zhao Y, Chen S & Owyang C (2006). Ghrelin acts on the dorsal vagal complex to stimulate pancreatic protein secretion. *Am J Physiol Gastrointest Liver Physiol* **290**, G1350–G1358.

Maccarinelli G, Sibilia V, Torsello A, Raimondo F, Pitto M, Giustina A, Netti C & Cocchi D (2005). Ghrelin regulates proliferation and differentiation of osteoblastic cells. *J Endocrinol* **184**, 249–256.

Mousseaux D, Le Gallic L, Ryan J, Oiry C, Gagne D, Fehrentz JA, Galleyrand JC & Martinez J (2006). Regulation of ERK1/2 activity by ghrelin-activated growth hormone secretagogue receptor 1A involves a PLC/PKCvarepsilon pathway. *Br J Pharmacol* **148**, 350–365.

Nakazato M, Murakami N, Date Y, Kojima M, Matsuo H, Kangawa K & Matsukura S (2001). A role for ghrelin in the central regulation of feeding. *Nature* **409**, 194–198.

Nogueiras R, Tovar S, Mitchell SE, Rayner DV, Archer ZA, Dieguez C & Williams LM (2004). Regulation of growth hormone secretagogue receptor gene expression in the arcuate nuclei of the rat by leptin and ghrelin. *Diabetes* **53**, 2552–2558.

Proks P & Ashcroft FM (2009). Modeling K(ATP) channel gating and its regulation. *Prog Biophys Mol Biol* **99**, 7–19.

Quick J, Ware JA & Driedger (1992).The structure and biological activities of the widely used protein kinase inhibitor, H7, differ depending on the commercial source. *Biochem Biophys Res Commun* **187**, 657–663.

Rossi F, Castelli A, Bianco MJ, Bertone C, Brama M & Santiemma V (2009). Atherosclerosis ghrelin inhibits contraction and proliferation of human aortic smooth muscle cells by cAMP/PKA pathway activation. *Atherosclerosis* **203**, 97–104.

Saito T (2006). In vivo electroporation in the embryonic mouse central nervous system. *Nat Protoc* **1**, 1552–1558.

Sakata I, Yamazaki M, Inoue K, Hayashi Y, Kangawa K & Sakai T (2003). Growth hormone secretagogue receptor expression in the cells of the stomach-projected afferent nerve in the rat nodose ganglion. *Neurosci Lett* **342**, 183–186.

Schwartz MW, Seeley RJ, Campfield LA, Burn P & Baskin DG (1996). Identification of targets of leptin action in rat hypothalamus. *J Clin Invest* **98**, 1101–1106.

Shi L, Bian X, Qu Z, Ma Z, Zhou Y, Wang K, Jiang H & Xie J (2013). Peptide hormone ghrelin enhances neuronal excitability by inhibition of Kv7/KCNQ channels. *Nat Commun* **4**, 1435.

Smith GP, Jerome C & Norgren R (1985). Afferent axons in abdominal vagus mediate safety effect of cholecystokinin in rats. *Am J Physiol Regul Integr Comp Physiol* **249**, R638–R641.

Suzuki M, Sasaki N, Miki T, Sakamoto N, Ohmoto-Sekine Y, Tamagawa M, Seino S, Marbán E & Nakaya H (2002). Role of sarcolemmal K(ATP) channels in cardioprotection against ischemia/reperfusion injury in mice. *J Clin Invest* **109**, 509–512.

Swartz EM, Browning KN, Travagli RA & Holmes GM (2014). Ghrelin increases vagally mediated gastric activity by central sites of action. *Neurogatroenterol Motil* **26**, 272–282.

Tack J, Depoortere I, Bisschops R, Delporte C, Coulie B, Meulemans A, Janssens J & Peeters T (2006). Influence of ghrelin on interdigestive gastrointestinal motility in humans. *Gut* **55**, 327–333.

Tschöp M, Flora DB, Mayer JP & Heiman ML (2002). Hypophysectomy prevents ghrelin-induced adiposity and increases gastric ghrelin secretion in rats. *Obes Res* **10**, 991–999.

Wang L, Chen Q, Li G & Ke D (2012). Ghrelin stimulates angiogenesis via GHSR1a-dependent MEK/ERK and PI3K/Akt signal pathways in rat cardiac microvascular endothelial cells. *Peptides* **33**, 92–100.

Yule DI & Williams JA (1992). U73122 inhibits Ca2+ oscillations in response to cholecystokinin and carbachol but not to JMV-180 in rat pancreatic acinar cells. *J Biol Chem* **267**, 13830–13835.

Zarbin MA, Wamsley JK, Innis RB & Kuhar MJ (1981). Cholecystokinin receptors: presence and axonal flow in the rat vagus nerve. *Life Sci* **29**, 697–705.

Zhou SY, Lu Y, Song I & Owyang C (2011). Inhibition of gastric motility by hyperglycemia is mediated by nodose ganglia K_{ATP} channels. *Am J Physiol Gastrointest Liv Physiol* **300**, G394–G400.

Additional information

Competing interests

The authors have no competing interests to declare.

Author contributions

GG and CO conceived and designed the experiments. GG, XW, YL, AH, IS, S-YZ and CO were responsible for the collection, analysis and interpretation of data. GG and CO drafted the article and revised the manuscript critically for important intellectual content.

Funding

This study was supported by the National Institute of Diabetes and Digestive and Kidney Diseases Grants R01 DK48419 (CO), R01 DK 84039 (CO) and P30 DK34933 (CO).

Supporting information

The following supporting information is available in the online version of this article.

Figure S1 *A*, Western blot showing that ghrelin stimulates nodose ganglia p-PI3K in a dose-dependent manner. *B*, Western blot shows that ghrelin stimulates nodose ganglia p-Erk1/2 in a dose-dependent manner. *C*, Western blot showing that ghrelin (20 nM)-stimulated p-Erk1/2 was inhibited by wortmannin (100 mM) and pertussis toxin (PTx, 1 U mL^{-1}) but not by PLC inhibitor U72133 (10 μM), PKC inhibitor calphostin C (1 μM), adenyl cyclase SQ22536 (100 μM) in the nodose ganglia. *D*, Western blot showing that ghrelin-stimulated Erk1 and Erk2 mRNA expression in vagal ganglia 96 h after transfection with random but not with PI3K siRNA.